Growth and characterization of AlGaAs/GaAs quantum well infrared photodetectors

H. ALTUNTAS*, S. OZCELIK
Gazi University, Department of Physics, 06500, Teknikokullar, Ankara, Turkey

Two AlGaAs/GaAs quantum well infrared photodetectors (QWIPs) were grown using molecular beam epitaxy (MBE) with continues growth method. One of them has bound-to-bound transition (B-T-B) QWIP and the other has bound-to-continuum transition (B-T-C) QWIP. The structural properties of the QWIPs were characterized by high-resolution x-ray diffraction (HRXRD) and optical properties were characterized by photoluminescence (PL) measurements. Also dark current measurements of the QWIPs were performed at low temperature and show that the B-T-C QWIP has lower dark current level than B-T-B QWIP due to reducing the carrier tunneling.

(Received May 04, 2009; accepted February 02, 2010)

Keywords: AlGaAs/GaAs QWIP, High resolution x-ray diffraction, Photoluminescence, Dark current

1. Introduction

Quantum-well infrared photodetectors (QWIPs) are based on intersubband transitions and they have been widely investigated during the past years [1-7]. QWIPs with longer wavelengths would be of interest for space applications such as infrared astronomy and satellite mapping where high detectivity, low dark current, high uniformity, radiation hardness and low power consumption are important. Also QWIPs are very important for 3-5 μm and 8- 12 μm atmospheric transmission windows because in these wavelengths atmosphere is transparent. Quantum well is created by low band gap material is sandwiched between the high band gap materials. Thus, quantize subbands are formed in the quantum well. Coming infrared radiation to QWIP excites the electrons in the well and excited electrons can transition to another state if infrared radiation energy is equal the difference between the subband states. Transition occurs between two bound state in quantum well, so called bound-to-bound transition (B-T-B), or transition occurs from bound state to continuum state (above conduction band), so called bound-to-continuum transition (B-T-C).

There are many types of QWIPs. But, lattice matched GaAs/AlGaAs QWIPs have attracted much attention because mature molecular beam epitaxy (MBE) growth and processing technologies, lead to devices with high uniformity, high yield, low cost, and other advantages [8, 9]. To obtain a high performance QWIP, the quality of quantum well must be controlled carefully. MBE has been successfully used to prepare various kinds of multi-layer structures, including multi-quantum wells and superlattices. One of the most important parameters of the QWIPSs is dark current level. Because the detectivity of infrared detectors is strongly dependent on the dark current, QWIPs structures have been designed to reduce the dark current level [10-11].

In this study, two AlGaAs/GaAs QWIP samples were grown by using MBE. The quantum well thicknesses are 55 Å and 45 Å for sample A and sample B, respectively. Hence, Sample A has bound-to-bound intersubband transition and sample B has bound-to-continuum transition. These transitions effect on dark current level of detector samples was discussed. Also, grown samples are characterized by high resolution x-ray diffraction (HRXRD) and photoluminescence (PL).

2. Experimental procedure

AlGaAs/GaAs QWIP samples were grown on epi-ready semi-insulating (SI) GaAs substrate with solid-source V80H- MBE system. Arsenic was supplied in the form of As_2 from a valved cracker cell. The substrates were outgassed at 400 °C for two hours in a preparation chamber before oxide desorption was performed by heating up to 590 °C with As_2 flux irradiation in the growth chamber. Substrates temperature during the growth was 570 °C and 560 °C for buffer layer and epilayers, respectively. Si was incorporated as n-type dopant and its cell temperature was 1150 °C.

A single period of multi-quantum well structure consists of GaAs well (doped $n \approx 8\times10^{17} cm^{-3}$) and AlGaAs barrier. Stacking identical quantum wells (50 times) together increases photon absorption. Ground state electrons are provided in the detector by doping the GaAs well layers with Si. These multi-quantum well layers are sandwiched between 500 nm n-doped GaAs top and 1000 nm n-doped GaAs bottom contact layers. Structures of the QWIP samples are shown in Fig. 1.

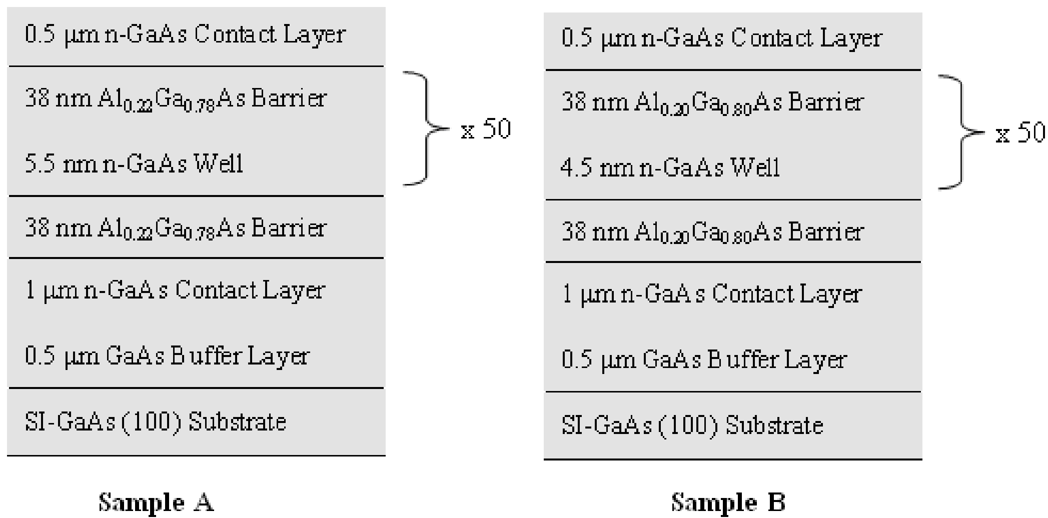

Fig.1. Structures of the AlGaAs/GaAs QWIPs.

The MBE grown QWIP structures were processed into 150 μm diameter mesa test structure using CCl_2F_2 RIE etching, and Au/Ge ohmic contacts were evaporated onto the top and bottom contact layers. Device pictures of the QWIPs are shown in Fig. 2.

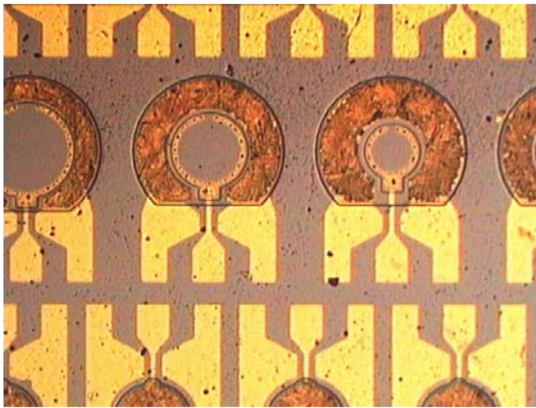

Fig. 2. Device pictures of the QWIPs.

3. Results and discussion

High resolution x-ray diffraction (HRXRD) has provided to be most popular tool the measure the epitaxial layer composition, thickness, strains, and structural properties. HRXRD from the QWIP samples was performed using a Bruker D8- Discover diffractometer, delivering a Cu Kα1 line. Fig. 3 shows the measured and simulated x-ray rocking curves of AlGaAs/GaAs QWIP structures. The simulation of HRXRD scan data was performed with the commercial software Leptos 1.07 by using simulating annealing method [12].

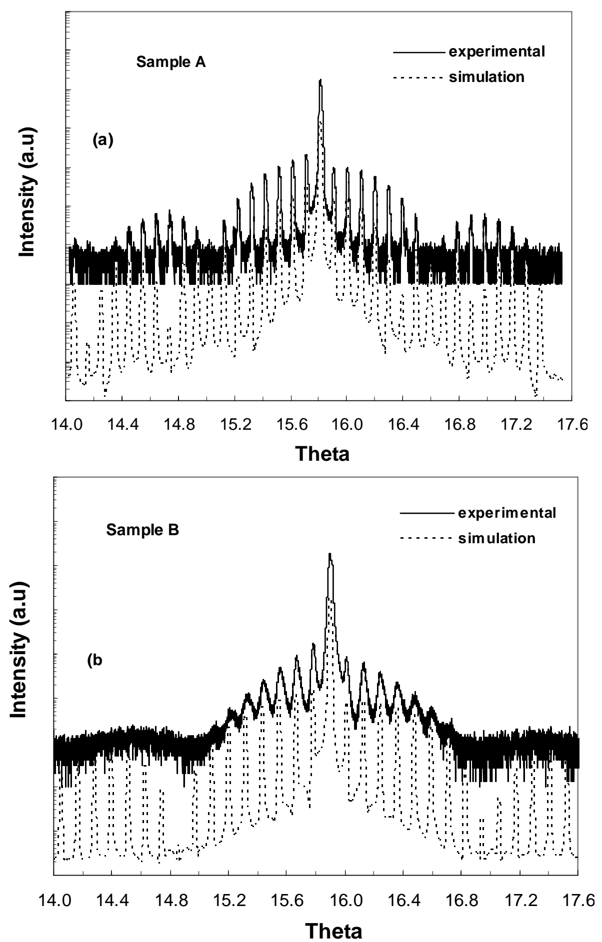

Fig. 3 (a) and (b). HRXRD profile of QWIPs samples along with simulation curves for sample A and sample B, respectively.

From Fig. 3 (a), a set of higher-order satellite peaks for Sample A QWIP structure are can be seen clearly. But for Sample B QWIP, higher-order satellite peaks are not discernible on the x-ray rocking curve with decreasing intensities. This usually results from the a little difference in lattice parameters between GaAs and AlGaAs layers and small thickness of the GaAs well compared with the AlGaAs barrier, and related to GaAs and AlGaAs interface quality. The peak with maximum intensity (GaAs substrate and buffer)'s full width at half maximum (FWHM) values are 63.38 and 98.64 arcsec. for Sample A and Sample B, respectively. The evaluation of FWHM X-ray peaks from the HRXRD is important since some quantities are quite often used as a first indication of the structural quality of epitaxial layers and superlattices [13]. The thicknesses of the well and barriers were obtained from the simulation data and they were given in Fig. 1.

Fig. 4 (a) and (b) show room temperature (RT) PL spectrum of AlGaAs/GaAs QWIP structures. A very strong PL band peaked at 1.498 eV for Sample A, comes from the fundamental recombination E_o between the ground states of the electron in the conduction subband and the heavy hole in the valance subband of the GaAs well. This transition value is very close to 1.49 eV that is theoretical value obtained from solving Poisson equation [14, 15]. Calculated energy levels are given in Table 1. The full width at half maximum (FWHM) is 27 meV. The inset figure in the Sample A PL, shows the peak at 1.704 eV (728 nm) is due to the recombination from AlGaAs barriers. By the expression of the $Al_xGa_{1-x}As$ energy bandgap

$$E_g\ (Al_xGa_{1-x}As) = E_g(GaAs) + 1.247x$$

we obtained the x value (composition rate) as 0.22. Here $E_g(GaAs)$ =1.424 eV is the bandgap of GaAs at room temperature. From RT PL spectrum for Sample B, x value was found as 0.20 and FWHM was 24 meV. The intensity of the E_o transition was stronger than AlGaAs. This strength is due to carrier confinement in the multiple quantum wells.

Table 1. Calculated energy level in QWIPs.

Sample	Barrier potential	First State(meV)	Second State(meV)	Transition
A	173.8	48	169	B-T-B
B	158	59	---	B-T-C

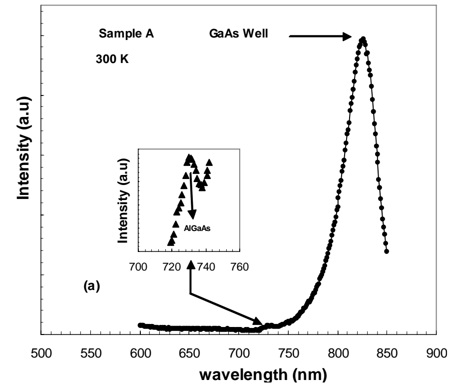

(a)

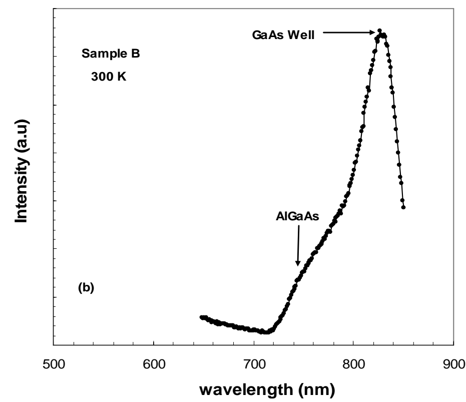

(b)

Fig. 4. Room temperature PL spectrum of QWIPs.

Fig. 5 (a) and (b) show conduction band diagram of B-T-B QWIP and B-T-C QWIP, respectively. As can be seen from Fig. 5 (a), transition occurs in two bound states, namely bound-to-bound transition. In B-T-B QWIPs, the excited carriers can tunneling through the barrier.

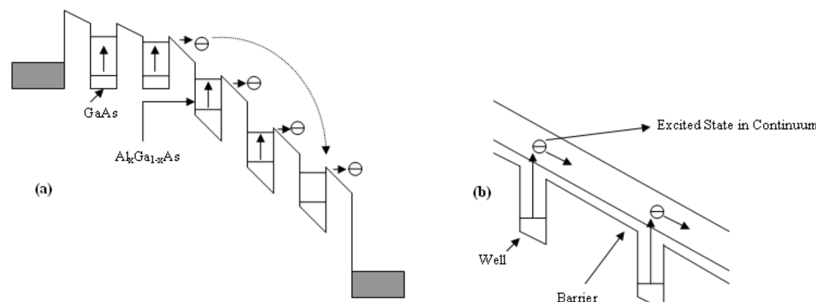

Fig. 5. Conduction band diagram of B-T-B QWIP (a) and B-T-C QWIP (b), [16].

Tunneling of the carriers from the well causes the dark current. By reducing quantum well width, bound-to-continuum intersubband absorption can be obtained. The main advantage of bound-to continuum QWIP is that the photoexcited electron can escape from the quantum well to the continuum conduction states without tunneling through the barrier as shown in Fig.5(b). In B-T-B QWIPs, ground state tunneling causes additional dark current [16].

Fig. 6 shows dark current-voltage characteristics of QWIPs. As can be seen from Fig. 6, dark current level of Sample B is much lower than Sample A due to Sample B QWIP has bound-to-continuum transition.

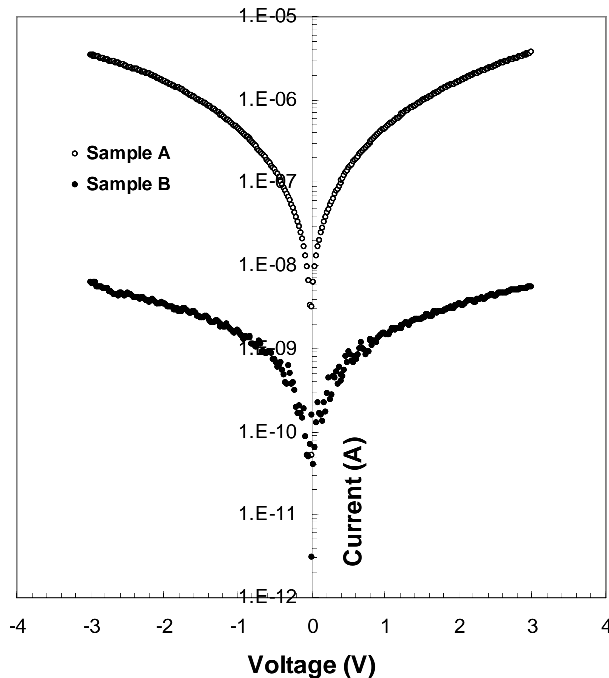

Fig. 6. Dark-current versus voltage characteristics of QWIPs.

As a result, in this study, bound-to-bound QWIP and bound-to-continuum QWIPs were characterized by HRXRD, PL, and dark current-voltage measurements. Although, B-T-C QWIP has less structural quality than B-T-B QWIP, B-T-C QWIP has lower dark-current level due to reducing the carrier tunneling.

Acknowledgments

The authors would like to thank Nanotam from Bilkent University for device fabrication. This study is supported by the DPT under project no 2001K120590.

References

[1] B. F. Levine, G. Hasnain, C. G. Bethea, N. Chand, Appl. Phys. Lett. **54**, 2704 (1989).
[2] B. F. Levine, C. G. Bethea, G. Hasnain, V. O. Shen, E. Pelve, R. R. Abbott, S. J. Hseih, Appl. Phys. Lett. **56**, 851 (1990).
[3] S. D. Gunapala, S. V. Bandara, K. C. Liu, W. Hong, M. Sundaram, P. D. Maker, R. E. Muller, C. A. Shott, R. Carrelejo, IEEE Transactions on Electron Devices **45**, 1890 (1998).
[4] B. F. Levine, Journal of Appl. Phys. **74**, R1 (1993).
[5] W. F. Wan, H. J. Qu, W. Lu, Q. Liu, S. O. Shen, N. Li, S. C. Shen, W. X. Wang, Q. Huang, J. Q. Zhou, Journal of Inf. and Millimeter Waves **17**, 76 (1998).
[6] W. Z. Shen, Journal of Inf. and Millimeter Waves **21**, 1739 (2000).
[7] N. Li, W. Lu, Q. Liu, Journal of Inf. and Millimeter Waves **19**, 25 (2000).
[8] H. C. Liu, J. M. Li, J. R. Thompson, Z. R. Wasilewski, M. Buchanan, J. G. Simmons, MEE Electron Device Lett. **14**, 566 (1993).
[9] Y. H. Zhang, D. S. Jians, J. B. Xia, L. Q. Cui, C. Y. Song, Z. Q. Zhou, W. K. Ge, Appl. Phys. Lett. **68**, 2114 (1996).
[10] Y. H. Wang, S. S. Li, J. Chu, Appl. Phys. Lett. **64**, 727 (1994).
[11] K. K. Choi, M. Z. Tidrow, M. Taysing-Lara, W. H. Chang, C. H. Kuan, C. W. Farley, F. Chang, Appl. Phys. Lett. **63**, 908 (1993).
[12] LEPTOS user manual, M 88-E02052, Version 2, Issue: June 17, 2004.
[13] Optical characterization of epitaxial semiconductor layers, Günther Bauer-Wolfgang Richter (Eds), 1996.
[14] G. L. Snider, I.-H. Tan, E. L. Hu, Journal of Appl. Phys. **68**, 2849 (1990).
[15] I.-H. Tan, G. L. Snider, E. L. Hu, Journal of Appl. Phys. **68**, 4071 (1990).
[16] S. D. Gunapala, S. V. Bandara, Semiconductors and Semimetals **62**, (1999).

*Corresponding author: ahalit@gazi.edu.tr